EARTHQUAKE ENGINEERING AND STRUCTURAL DYNAMICS
Earthquake Engng Struct. Dyn. (in press)
Published online in Wiley InterScience (www.interscience.wiley.com). DOI: 10.1002/eqe.657

Case studies of damage to 19-storey irregular steel moment-frame buildings under near-source ground motion

Swaminathan Krishnan*, †

Seismological Laboratory, MS 252-21, California Institute of Technology, Pasadena, CA 91125, U.S.A.

SUMMARY

This paper describes the three-dimensional nonlinear analysis of six 19-storey steel moment-frame buildings, designed per the 1997 Uniform Building Code, under strong ground motion records from near-source earthquakes with magnitudes in the range of 6.7–7.3. Three of these buildings possess a reentrant corner irregularity, while the remaining three possess a torsional plan irregularity. The records create drift demands of the order of 0.05 and plastic rotation demands of the order of 4–5% of a radian in the buildings with reentrant corners. These values point to performance at or near 'Collapse Prevention'. Twisting in the torsionally sensitive buildings causes the plastic rotations on the moment frame on one face of the building (4–5% of a radian) to be as high as twice of that on the opposite face (2–3% of a radian). The asymmetric yield pattern implies a lower redundancy in the lateral force-resisting system as the failure of the heavily loaded frame could result in a total loss of resistance to torsion. Copyright © 2006 John Wiley & Sons, Ltd.

Received 14 December 2005; Revised 30 September 2006; Accepted 2 October 2006

KEY WORDS: tall buildings; moment-frames; near-source ground motion; irregularity

1. INTRODUCTION

Near-source ground motion is characterized by rapidly occurring (i.e. high velocity) displacement pulses [1, 2]. The rapid velocity at which these displacements occur leads to pulses in the velocity time histories as well. The characteristic period of these pulses is typically in the range of 2–6 s which corresponds to the fundamental natural period range of 15–50 storey structures. Hall *et al.* [2] have studied the propagation of these pulses through the height of an idealized shear building as a wave. The velocity pulse produces a shear wave that causes a velocity-proportional strain in

*Correspondence to: Swaminathan Krishnan, Seismological Laboratory, MS 252-21, California Institute of Technology, Pasadena, CA 91125, U.S.A.
†E-mail: krishnan@caltech.edu

Contract/grant sponsor: California Institute of Technology

the structure. The wave has a forward pulse and a reverse pulse. The constructive interference of these pulses travelling up and down the building results in yield localization and the formation of a kink in the building. Such a kink could cause large P–Δ effects compromising the stability of the structure. Using simplified assumptions, such as a uniform shear building and an idealized ground motion pulse, it is possible to predict when and where along the height of the structure this kink is likely to occur. However, for real buildings, especially of the irregular kind, subjected to three-component ground motion, it would be practically impossible to use wave theory to determine the extent and distribution of yielding. The only alternative is to build a detailed three-dimensional finite-element model of the building.

Near-source ground motion from large earthquakes has been recorded only in recent times. Their effects on both regular and irregular tall buildings are virtually unknown. Near-source factors have been introduced in the 1997 Uniform Building Code, UBC97 [3] to account for some of the special features of near-source ground motion (it should be pointed out that the more recent International Building Code, IBC2006 [4], does not explicitly specify near-source factors for near-source conditions; higher ground motions at sites close to active faults are specified in the maximum considered earthquake ground motion maps instead). Due to lack of data at this stage, it is not clear how buildings designed according to these guidelines will fare in a near-source event. This raises many fundamental questions that need to be carefully addressed: what is the ductility demand on code-designed tall buildings under near-source ground motion similar to what has been recorded in recent times during the 1994 Northridge earthquake, the 1995 Kobe earthquake, and the 1999 Turkey and Taiwan earthquakes? What kind of interstorey drifts and permanent roof offsets can be expected during such events? How do irregular features in the building contribute to overall building damage? One way of addressing these questions is to conduct inelastic dynamic time-history analyses of structural models of a carefully selected suite of irregular buildings subject to recorded strong ground motion from a suite of near-source earthquake records. Since building designs, especially of the irregular kind, designed according to UBC97 are not readily available, four 19-storey steel moment-frame buildings, labelled B-1 through B-4, are designed based on these provisions. Buildings B-1 and B-2 have reentrant corners while buildings B-3 and B-4 have a plan torsional irregularity. The irregular features in buildings B-2 and B-3 are such that the frames have to be considerably stiffened (and as a result strengthened) to satisfy empirical wind drift limits. Such limits are generally imposed by practising engineers to ensure occupant comfort and the safety of non-structural components (facades, etc.). Since building codes generally do not require adherence to a wind drift limit, it is possible that buildings are being designed without the imposition of a wind drift limit. It is of interest to compare the performance of such buildings against those that adhere to a wind drift limit. With this objective, buildings B-2 and B-3 are redesigned to withstand earthquake and wind loads but only the earthquake drifts were controlled to code-specified values. These variants of buildings B-2 and B-3 are labelled B-2A and B-3A, respectively.

2. BUILDING DESCRIPTION AND DESIGN DETAILS

Buildings B-2 and B-3, and their variants B-2A and B-3A, are designed as office buildings. Building B-1 is designed for residential purposes while building B-4 is a commercial mixed-use structure with hotel occupancy on the lower floors and office occupancy on the upper floors. The fundamental periods of all the buildings are strictly constrained to lie between 3.2 and 3.5 s during

DOI: 10.1002/eqe

the design process making it possible to compare the performance of the buildings against each other. Also, the conclusions drawn from the computationally generated data set pertaining to this narrow class of buildings would be reliable. All the buildings are assumed to be located in Seismic Zone 4 (UBC97 [3]) at a distance of 5 km from a Type A fault. The soil at the site is assumed to be of Type S_b per the UBC97 soil classification. Linear dynamic response spectral analysis is performed on three-dimensional linear elastic models of the six buildings using the commercial program ETABS [5]. For wind design, the buildings are assumed to be located in an area that is categorized as Exposure B in UBC97 [3].

2.1. Buildings with reentrant corners

A brief description of all the buildings along with the floor plans and isometric views are given in the next two sections. The elevations (labelled on plan) of the moment-frames and gravity columns, beam and column sizes, and building characteristics, such as the location of the centres of mass and stiffness, are given in Reference [6]. ASTM-A572, Grade 50 steel is used for the beams and columns in all the buildings. It is assumed that the nominal yield stress is 344.85 MPa (50 ksi) and the nominal ultimate stress is 448.31 MPa (65 ksi). The primary lateral system consists of steel moment frames. The floors are made of concrete slab on metal deck (14 cm thick with 2.5 cm topping) supported by steel beams framing into columns. The interior floor-framing beams are assumed pinned at both ends and their contribution to the overall stiffness and strength of the lateral force-resisting system is neglected.

Building B-1 is dumbbell-shaped in plan (Figure 1(a)) with two elevator cores to serve the two spines of the building. The presence of setbacks precludes multiple-bay moment frames along the perimeter. However, there are two 3-bay moment-frames (along grids C and D) in the building long direction (X) and one 5-bay moment-frame (along grid 4) in the building short direction (Y). Typical storey height is 3.6 m with variations at the lobby and the mechanical stories. The isometric view of the building is illustrated in Figure 1(b). The dark lines represent the moment-frame beams and columns. The grey rectangles represent the floor slab. The single-bay frames on the building perimeter lead to the building being torsionally soft in addition to reducing the redundancy in the system by forcing the 5-bay frame in the Y-direction and the two 3-bay frames in the X-direction to carry majority of the seismic shear. Although the building does not have any axis of symmetry, it does possess a certain kind of geometric symmetry. Both the centre of mass and the centre of stiffness lie at the midpoint of column line 4 (Figure 1(a)). This precludes twisting under seismic loading, unless the building yields unsymmetrically which is certainly possible because the two horizontal components of ground motion when applied simultaneously will cause an unsymmetrical load pattern on the beams and columns. The single-bay moment-frames are not very effective in sharing the seismic loads, thus lowering the overall redundancy of the system. The peak interstorey drift ratios due to the seismic design forces are well below the inelastic interstorey drift limit of 0.02.

Building B-2 is L-shaped in plan (Figure 1(c)) with one elevator core serving both wings of the building. In L-shaped buildings such as this, the wings, with fewer moment-frame bays, being less stiff have a tendency to flap during strong shaking. Out-of-phase shaking of the wings could lead to stress concentration at the reentrant corner and potential failure in a tearing mode. In-phase shaking of the wings could lead to twisting in the building and potential failure in a torsional mode. Typical storey height is 4.0 m with variations at the lobby and the mechanical stories. The isometric view of the building is illustrated in Figure 1(d). The wings have only two-bay moment-frames across

DOI: 10.1002/eqe

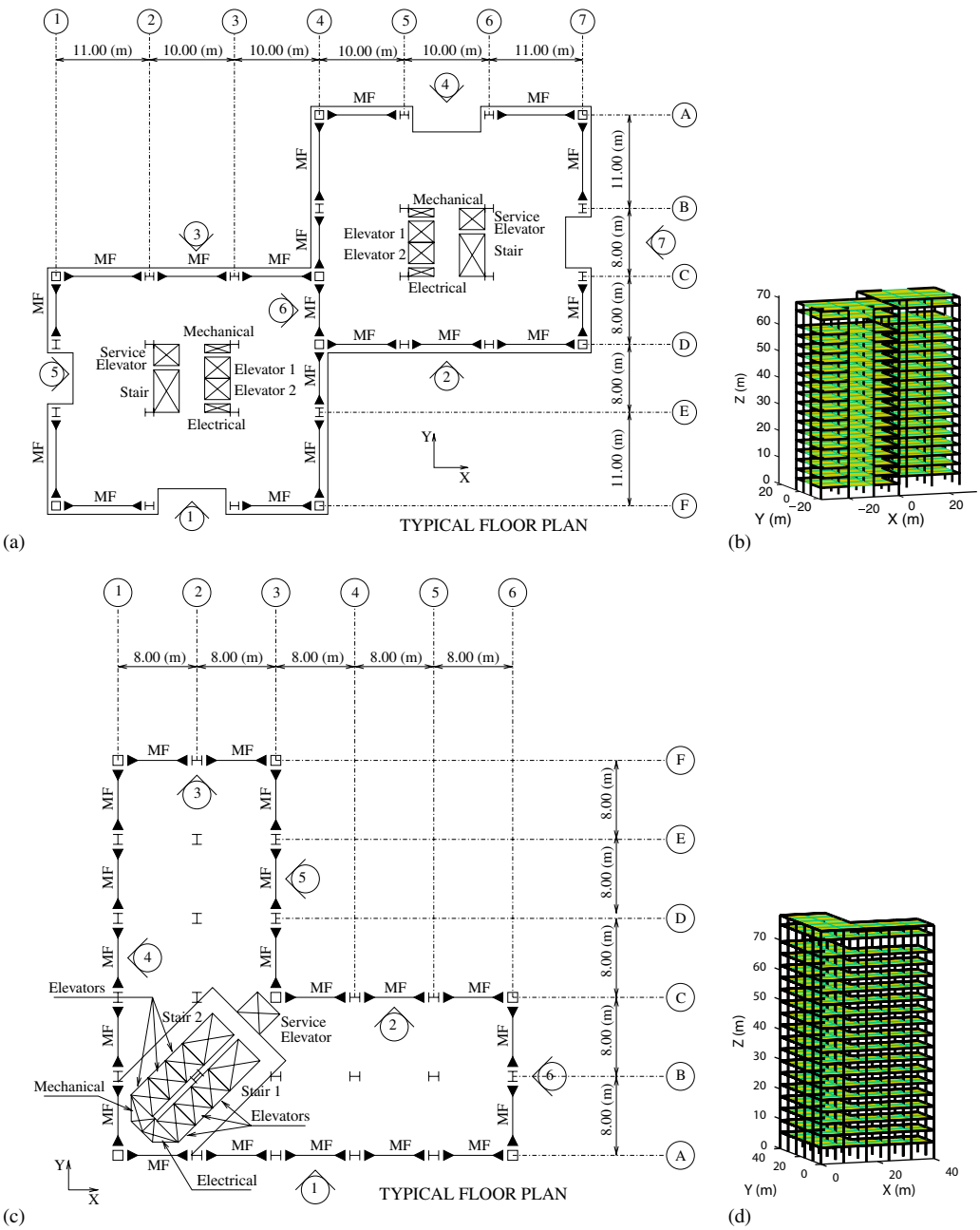

Figure 1. Buildings with reentrant corners: (a) typical floor plan of building B-1; (b) isometric view of building B-1; (c) typical floor plan of buildings B-2 and B-2A; and (d) isometric view of buildings B-2 and B-2A.

DOI: 10.1002/eqe

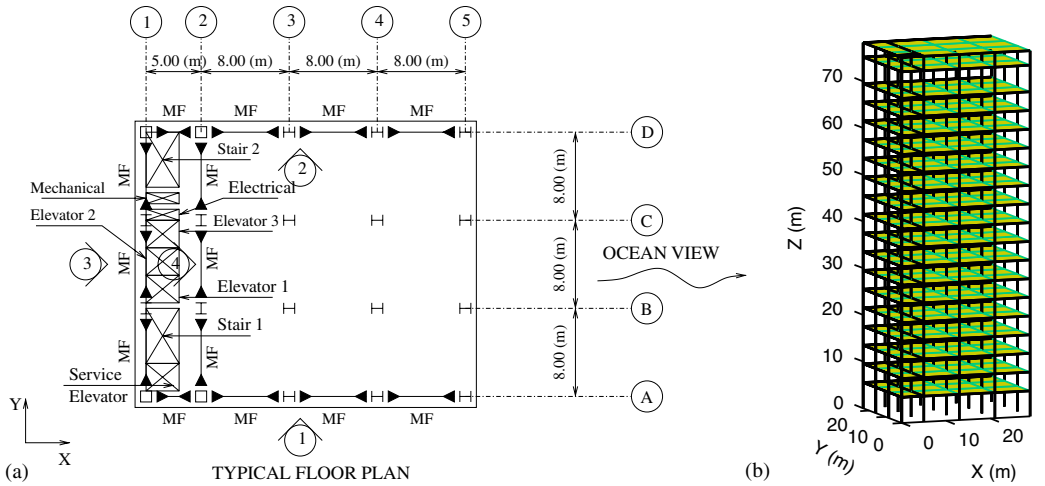

Figure 2. (a) Typical floor plan of buildings B-3 and B-3A; and (b) isometric view of buildings B-3 and B-3A.

their ends and, as a result, are softer than the spine (reentrant corner region) of the building. Wind forces control the design of the moment-frames at the wings. The centre of stiffness (on plan) of the building being closer to the reentrant corner than to the point of application of wind forces leads to twisting in the building under wind forces. Since the wings are soft, this torsion leads to large drifts at the far corners (at grid intersections F-1, F-3, C-6, and A-6 in Figure 1(c)). While reduction in the drift due to building translation (sway) is achieved by stiffening all moment-frames, reducing the drift in the short direction of the wings requires the stiffening of the beams and columns in the 2-bay moment-frames at the wings (frames 3 and 6 along grids F and 6 in Figure 1(c)) relative to those in the 3-bay and 5-bay moment-frames (frames 1, 2, 4, and 5 along grids 1, 3, A, and C, respectively). This moves the centre of stiffness from within the spine to a location very close to the reentrant corner. However, this remedial measure to distribute the stiffness (on plan) more uniformly is still not sufficient to eliminate twisting in the building under wind forces. But the reduction in the translational drift (sway) allows the wind drift at the far corners (at grid intersections F-1, F-3, C-6, and A-6 in Figure 1(c)) to be limited to 0.0025.

To arrive at the design of building B-2A starting from building B-2, the stiffness of the wing moment-frames as well as the spine moment-frames has been reduced in the same proportion. No wind drift limit is imposed in the design of building B-2A. By retaining the higher relative stiffness of the 2-bay frame in relation to the 3-bay and 5-bay frames, the centre of stiffness is held close to the reentrant corner even though there is a greater eccentricity in the locations of the centre of mass and centre of resistance relative to each other. Some columns are heavier than in building B-2 because of the increased P–Δ effects resulting from the reduction in the stiffness of the structure. Some amount of twisting is observed when wind loads are applied to the structure. This is due to the fact that the centre of application of wind forces is along the vertical centroidal axis of the projected area of the building in the path of the wind, while the centre of stiffness is closer to the reentrant corner leading to torsional eccentricity under wind loading. However, in the case of seismic forces, there is very little twisting observed consistent with the fact that the centres of mass and stiffness are located close to each other.

DOI: 10.1002/eqe

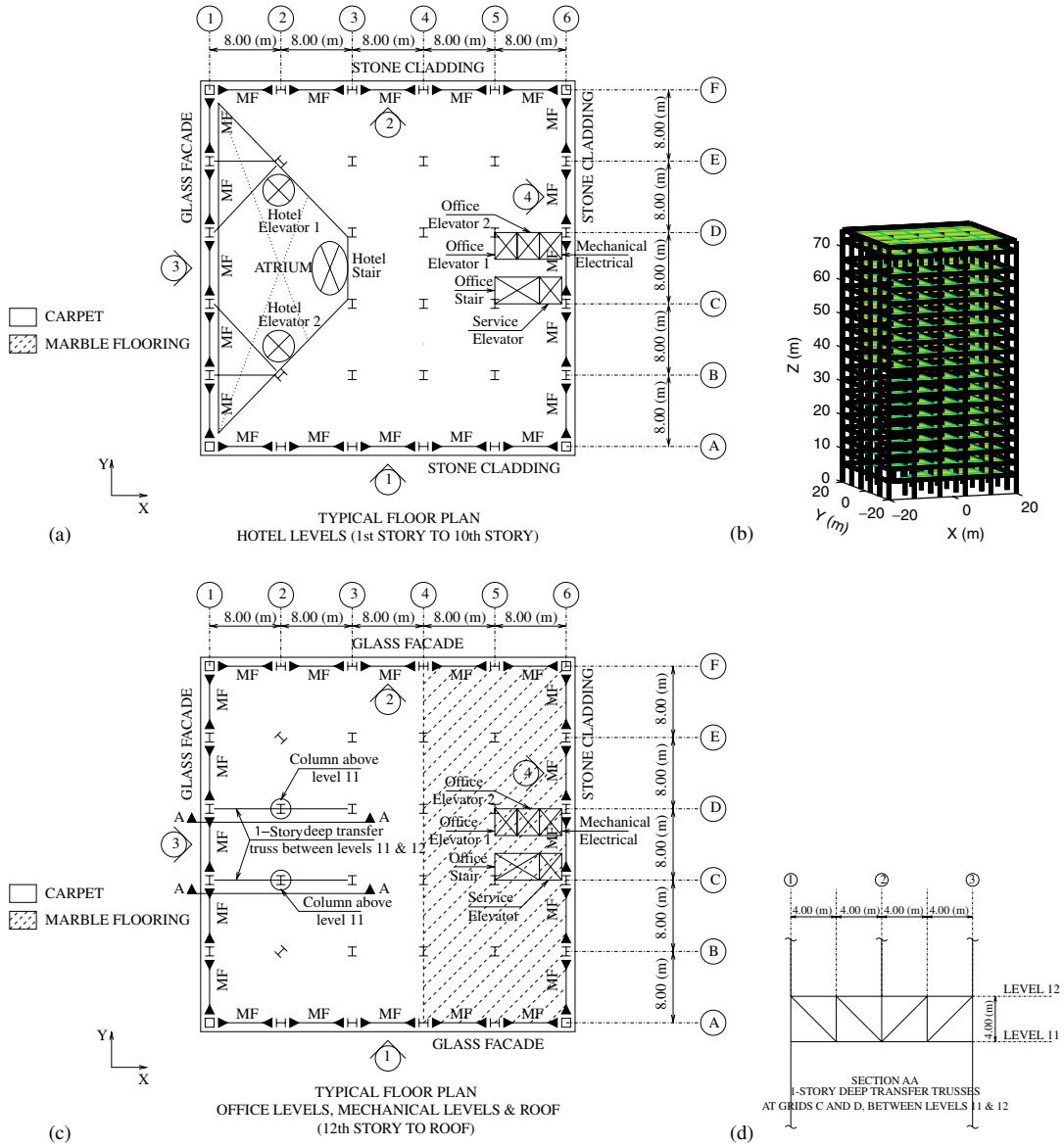

Figure 3. (a) Typical plan of hotel floors in building B-4; (b) isometric view of building B-4; (c) typical plan of office floors in building B-4; and (d) elevation of transfer truss in building B-4.

2.2. Buildings with torsional irregularity

Building B-3 is rectangular-shaped in plan (Figure 2(a)) with the elevators and stairs located along one face of the building. In order to transfer the diaphragm forces to and from the moment frame on grid 1, horizontal braces under the landings of the two stairs are required to act as collector elements. These are not shown on the plan. The ocean view on the building face along grid 5

DOI: 10.1002/eqe

Table I. Building natural periods and modal directions (first 3 modes).

Building ID	Mode number	Period (s)	Modal direction factors		
			X-translational	Y-translational	Z-rotational
B-1	1	3.50	91.55	3.61	4.84
	2	3.41	5.67	89.52	4.81
	3	2.69	2.77	6.88	90.35
B-2	1	3.39	50.00	50.00	0.00
	2	3.32	49.89	49.89	0.22
	3	2.33	0.12	0.12	99.76
B-2A	1	4.15	50.00	50.00	0.00
	2	4.11	49.93	49.93	0.14
	3	2.78	0.08	0.08	99.84
B-3	1	3.21	0.00	72.64	27.36
	2	2.03	100.00	0.00	0.00
	3	1.22	0.00	30.99	69.01
B-3A	1	4.74	0.00	79.16	20.84
	2	2.75	100.00	0.00	0.00
	3	1.85	0.00	20.91	79.09
B-4	1	3.49	0.00	96.67	3.33
	2	3.05	100.00	0.00	0.00
	3	1.91	0.00	3.51	96.49

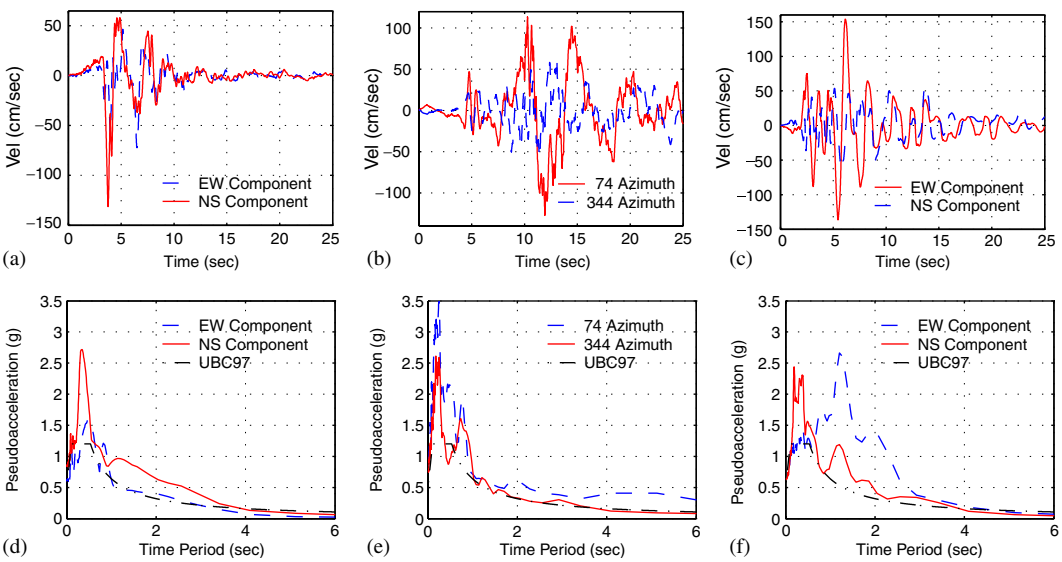

Figure 4. Horizontal components of Sylmar, Tabas, and Takatori ground motion records: (a) Sylmar velocity; (b) Tabas velocity; (c) Takatori velocity; (d) Sylmar pseudoacceleration response spectra; (e) Tabas pseudoacceleration response spectra; and (f) Takatori pseudoacceleration response spectra.

DOI: 10.1002/eqe

Table II. Ground motion analysis: building peak roof displacements (δ_{peak}^{roof}), peak interstorey drift ratios (Δ_{peak}), and permanent roof displacements (δ_{perm}^{roof}) in the direction of the strong component of the earthquake.

		Ground motion record					
Building ID	Response quantity	Sylmar $[X]^*$	Sylmar $[Y]^\dagger$	Tabas $[X]^*$	Tabas $[Y]^\dagger$	Takatori $[X]^*$	Takatori $[Y]^\dagger$
B-1	δ_{peak}^{roof} (m)	0.80	0.90	2.00	1.90	1.30	1.20
	Δ_{peak}	0.030	0.028	0.054	0.048	0.054	0.046
	δ_{perm}^{roof}	0.2	0.2	0.9	0.9	0.7	0.5
B-2	δ_{peak}^{roof} (m)	0.80	0.80	2.10	2.10	1.10	1.10
	Δ_{peak}	0.026	0.026	0.050	0.050	0.042	0.042
	δ_{perm}^{roof}	0.1	0.1	0.9	0.9	0.5	0.5
B-2A	δ_{peak}^{roof} (m)	0.75	0.75	2.30	2.30	0.85	0.85
	Δ_{peak}	0.030	0.030	0.053	0.053	0.047	0.047
	δ_{perm}^{roof}	0.1	0.1	0.8	0.8	0.2	0.2
B-3	δ_{peak}^{roof} (m)	0.95	1.20	1.20	2.00	1.40	1.50
	Δ_{peak}	0.024	0.033	0.023	0.033	0.043	0.040
	δ_{perm}^{roof}	0.1	0.3	0.3	0.3	0.4	0.4
B-3A	δ_{peak}^{roof} (m)	1.10	1.30	1.30	2.60	1.00	1.10
	Δ_{peak}	0.028	0.046	0.030	0.056	0.052	0.062
	δ_{perm}^{roof}	0.2	0.1	0.4	0.8	0.4	0.4
B-4	δ_{peak}^{roof} (m)	0.85	0.90	2.00	2.40	1.00	1.10
	Δ_{peak}	0.032	0.035	0.046	0.065	0.048	0.057
	δ_{perm}^{roof}	0.2	0.3	0.6	1.0	0.4	0.6

*Strong ground motion component in building's X direction.
†Strong ground motion component in building's Y direction.

precludes the use of deep beams that would restrict the view on that face. Thus, the moment-frame on that face had to be shifted to lie along grid 2. This creates a large open layout with maximum headroom for the offices between grids 2 and 5, and A and D with maximum beam depths being governed by gravity loads. The shifting of the moment-frame away from grid 5 to grid 2 shifts the centre of stiffness towards grid 2. On plan, the centre of mass is at about the centre of the building. This eccentricity between the locations of the centre of mass and the centre of stiffness leads to torsional sensitivity in the building. Note that the mass–stiffness eccentricity is only in one principal direction. Typical storey height is 4.0 m with variations at the lobby and the mechanical stories. The isometric view of the building is illustrated in Figure 2(b). For Y direction wind analysis, the centre of stiffness does not coincide with the centre of applied force and this leads to twisting in the building. There is considerably greater interstorey drift at the soft corners, A-5 and D-5, when compared to the stiff corners, A-1 and D-1. While the translational component

DOI: 10.1002/eqe

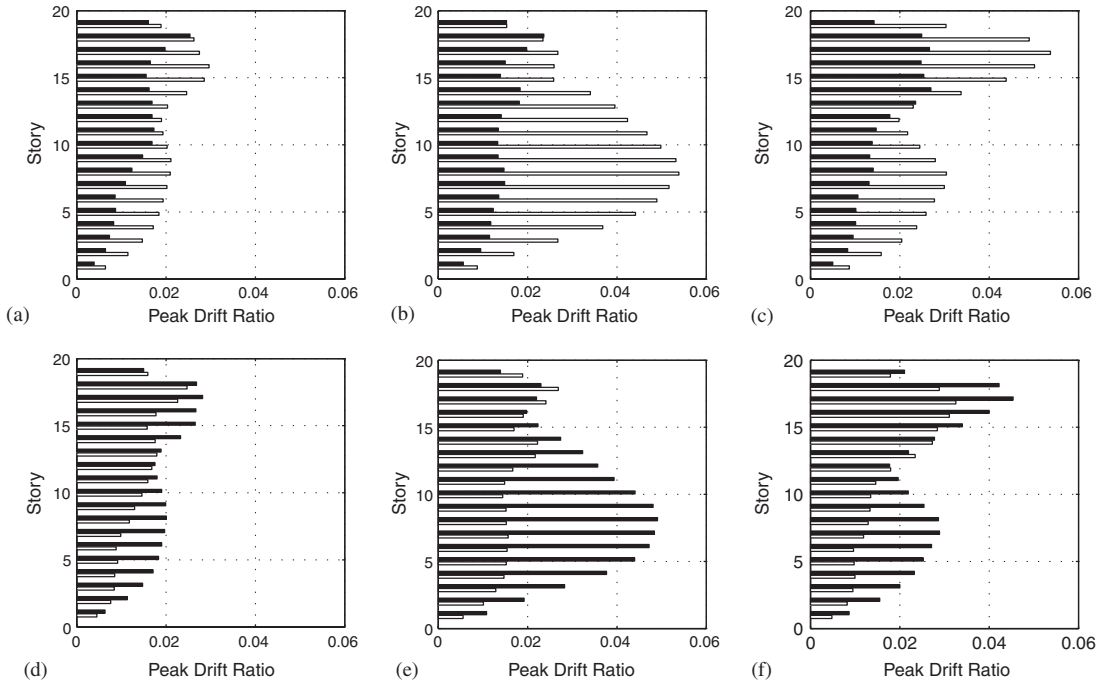

Figure 5. Building B-1 peak interstorey drifts (white bars represent X drifts and black bars represent Y drifts): (a), (b), and (c) Sylmar, Tabas, and Takatori record strong components in building's X direction; and (d), (e), and (f) Sylmar, Tabas, and Takatori record strong components in building's Y direction.

of the wind drift is resisted by the Y direction moment-frames along grids 1 and 2, the twisting component is primarily resisted by the X direction moment-frames along grids A and D. Thus, in order to restrict the overall drift to the generally accepted elastic wind drift limit of 0.0025, all four moment-frames had to be stiffened (and, as a result, strengthened). The Y direction wind drifts are quite high as a result of the unsymmetrical nature of the lateral force-resisting system in that direction [6]. In fact, they barely satisfy the imposed wind drift limit of 0.0025. Seismic drifts, on the other hand, are well below the code inelastic interstorey drift limit of 0.02. The system redundancy factor in the Y direction was close to the allowable limit of 1.25 for moment-frame buildings as a result of torsion loading the frames disproportionately. Building B-3A has the same plan and elevation as building B-3 (Figures 2(a) and (b)), except that it has been designed without any imposed wind drift limit. The stiffness of all four frames in building B-3A is reduced.

Building B-4 (Figure 3) is a 19-storey mixed-use tower (75.1 m tall) with a hotel in the lower 10 stories and an office in the upper nine stories. The hotel floors (Figure 3(a)) contain a large atrium. The presence of this opening shifts the centre of mass from the midpoint of the floor plan further away from the atrium face. Similarly, since architectural considerations limit the beam depth to 500 mm on the atrium face, the centre of stiffness is also shifted from the midpoint of the floor plan further away from the atrium face. However, the shift in the centre of stiffness is greater

DOI: 10.1002/eqe

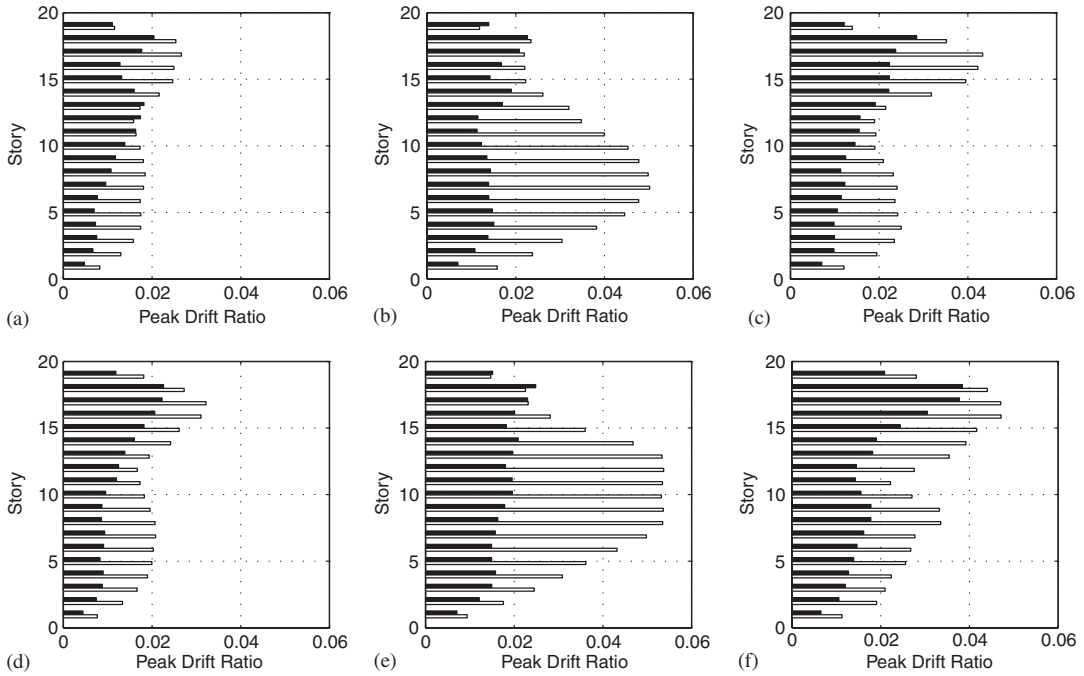

Figure 6. Peak interstorey drifts in buildings B-2 and B-2A (white bars represent *X* drifts and black bars represent *Y* drifts): (a)–(c) Sylmar, Tabas, and Takatori record strong components in building B-2 *X* direction; and (d)–(f) Sylmar, Tabas, and Takatori record strong components in building B-2A *X* direction; Since the buildings are symmetric, the results corresponding to the cases where the strong component of the ground motion is oriented in the building's *Y* direction can be inferred.

than the shift in the centre of the mass. This results in torsional eccentricity in the building. Note that the mass–stiffness eccentricity is unidirectional with only *Y* direction excitation being able to induce twisting in the building. The atrium at the lower (hotel) levels requires the termination of columns at grid intersections C-2 and D-2 at the 11th floor. The loads from these columns are transferred to the adjacent columns by way of one-storey deep, two-bay trusses along grids C and D, between grids 1 and 3. The elevation of these two transfer trusses is shown in Figure 3(d). At the atrium (hotel) levels, the columns of the moment frame along grid 1 are laterally braced by horizontal braces extending from columns at grid intersections, B-2 and E-2 (Figure 3(a)). These braces also serve to transfer some of the diaphragm forces to this frame. Even though this building seems highly irregular, it does not satisfy the UBC97 [3] torsional irregularity criteria and so has been designed as a regular building. Since the centres of mass and stiffness do not coincide, there is some amount of twisting observed in the response spectral analysis. Seismic drifts are well below the code-imposed drift limit of 0.02. In the *X* direction, the centre of stiffness coincides with the centre of the applied wind force. In the *Y* direction, on the other hand, there is a slight eccentricity between the centres of force and stiffness resulting from a 500 mm limit on the beam depth (architectural requirement) in the moment-frame adjacent to the atrium (along grid 1) that moves the centre of stiffness away from the atrium towards grid 6. The small eccentricity does not

DOI: 10.1002/eqe

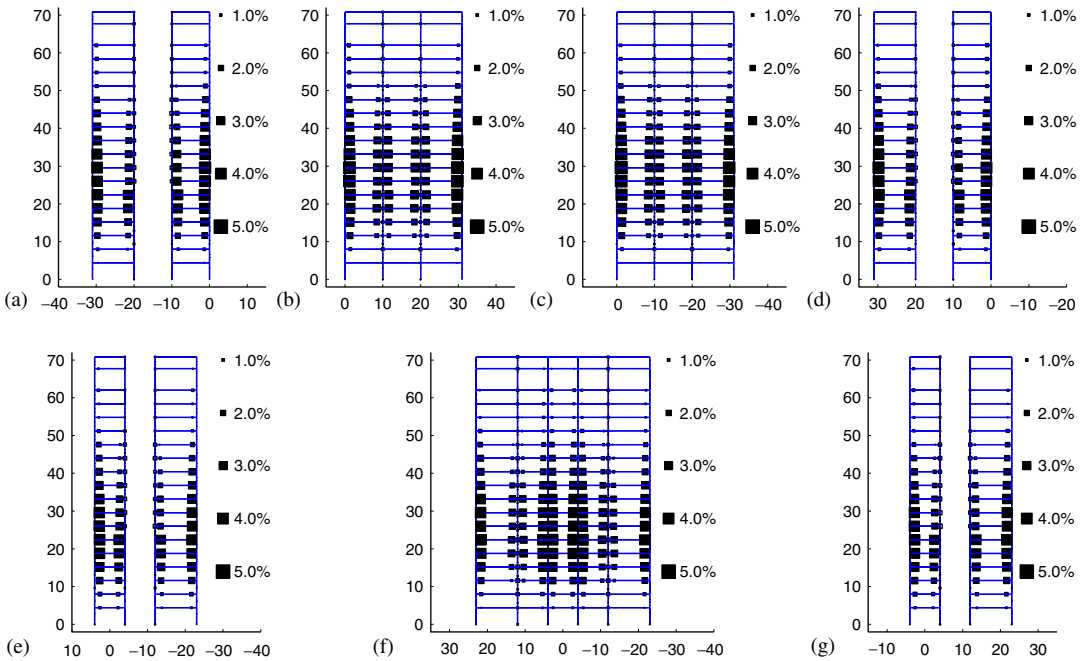

Figure 7. Plastic rotations at ends of beams and columns (black squares), and panel zones (white squares) in (a)–(d) frames MF-1 to MF-4 of building B-1 during shaking from the Tabas record with its strong component oriented in the building's X direction. Minor yielding occurs in the Y direction frames MF-5 to MF-7; and (e)–(g) frames 5–7 of building B-1 during shaking from the Tabas record with its strong component oriented in the building's Y direction. Minor yielding occurs in the X direction frames 1–4.

lead to significant twisting due to wind. Wind drifts are well below the imposed limit of 0.0025 which is a direct result of the efficient 5-bay moment-frames in either direction.

2.3. Dynamic characteristics of the buildings

The natural periods of the first three modes and the corresponding modal directions for all six buildings are given in Table I. While the first two modes of building B-1 are along its principal directions, the first two modes of buildings B-2 and B-2A are at an angle of 45° to their principal directions. In buildings B-3 and B-3A the X-translational and Z-rotational modes are coupled, although the X-translational mode is much stiffer than the Z-rotational mode in both cases. In contrast, there is little coupling between the X-translational and Z-rotational modes of building B-4. Consistent with the softer moment-frames in B-3A when compared to B-3, the first three natural periods of building B-3A are much longer than B-3.

3. ANALYSIS PRELIMINARIES, ASSUMPTIONS, AND LIMITATIONS

Nonlinear analyses of the buildings subjected to earthquake ground motion are performed using the building analysis program FRAME3D [7, 8]. Moment-frame beams and columns are

DOI: 10.1002/eqe

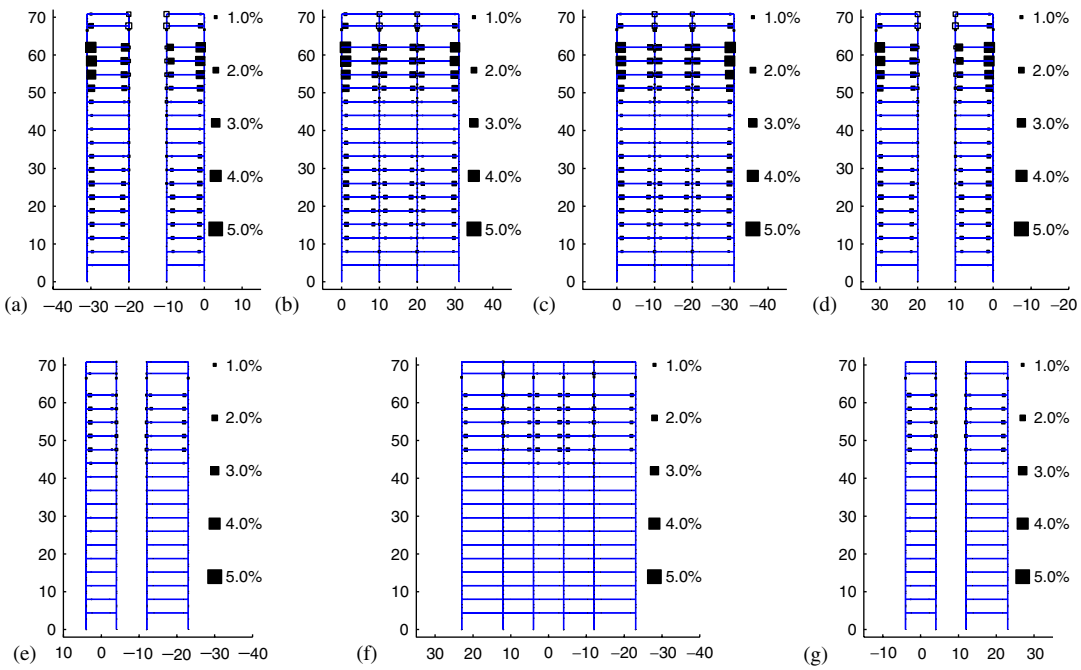

Figure 8. Plastic rotations at ends of beams and columns (black squares), and panel zones (white squares) in frames MF-1 to MF-7 of building B-1 during shaking from the Takatori record with its strong component oriented in the building's X direction.

modelled using elastofibre elements [9], beam–column joints using panel zone elements [10], and floor slabs using elastic plane-stress elements. Floor openings are not modelled. The elastofibre beam element is divided into three segments, with the interior segment being modelled as a cubic-interpolated displacement-based elastic beam and nonlinearity being restricted to the two exterior segments. These end segments are discretized in the cross-section into 20 fibres. The axial stress–strain behaviour of each fibre is governed by a backbone curve that resembles very closely the stress–strain curve obtained in a standard tension test of a steel rod in the laboratory. It consists of a linear elastic portion followed by a yield plateau leading to a strain-hardening region that is approximated using a cubic ellipse. Fibre yield and ultimate stresses are assumed to be 344.85 MPa (50 ksi) and 448.31 MPa (65 ksi), respectively. Fibre strain-hardening and rupture strains are assumed to be 0.012 and 0.16, respectively, while the slope at the initiation of strain-hardening is assumed to be 4000.26 MPa (580 ksi). The three-dimensional panel zone element consists of two orthogonal panels forming a cruciform section. The two flange plates of the joint portion of the column are combined to form panel 1 and the one or two web plates along with doubler plates, if any, are combined to form panel 2. The two panels can yield in shear. The shear stress–strain backbone curve for each panel consists of a linear portion followed by a quadratic portion to represent strain hardening. There is no distinct yield plateau which is

DOI: 10.1002/eqe

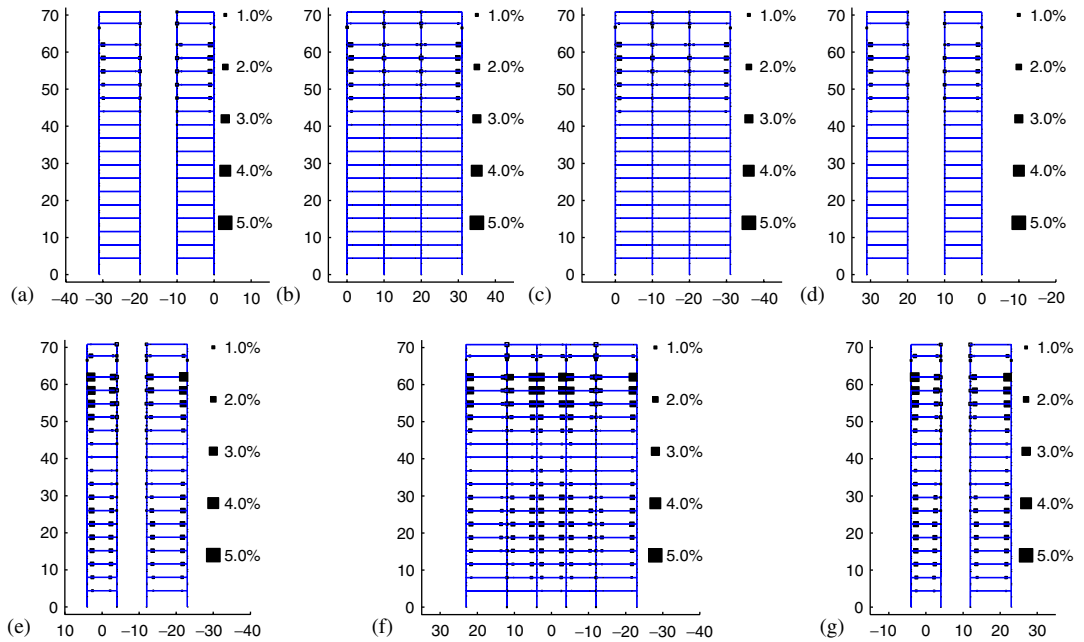

Figure 9. Plastic rotations at ends of beams and columns (black squares), and panel zones (white squares) in frames MF-1 to MF-7 of building B-1 during shaking from the Takatori record with its strong component oriented in the building's Y direction.

consistent with laboratory experiments on plates. In order to compute reactions at the base of the buildings, translational springs with large stiffness are placed at the base of all the columns. Foundations are not modelled. Soil–structure interaction is not included. Strength degradation in the various elements due to weld fracture, local flange buckling, or other means is not included. Thus, only the second order P–Δ effect can result in collapse of the structure. Column splices are not explicitly modelled. Composite action arising out of the shear connection between the concrete slab on metal deck and the moment-frame beams is not included. At each level, the storey mass is lumped at the location, on plan, of each column based on its tributary plan area. Thirty per cent of the live load is included along with the dead load in the lumped masses. An average of 30% of the live load is included in the gravity loads for ground motion analyses. Gravity columns are modelled using plastic hinge elements and their contribution to the P–Δ effects are automatically included. They are assumed continuous over the height of the building. Trusses and horizontal braces are assumed to be pinned at their ends. Elevator and stair openings are not modelled. The material properties of beam–column and panel zone elements are given in Reference [6]. Nominal strengths are used for all components. An effective thickness of 4 in is assumed for the plane-stress elements representing the concrete slab on metal deck.

DOI: 10.1002/eqe

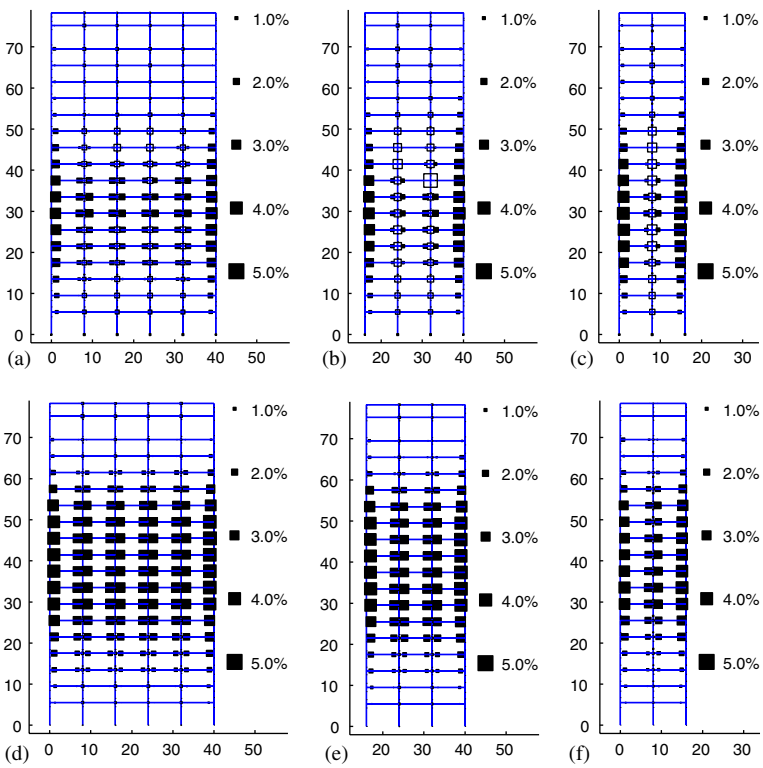

Figure 10. Comparison of plastic rotations at ends of beams and columns (black squares), and panel zones (white squares) in frames MF-1 to MF-3 of building B-2 against that in frames MF-1 to MF-3 of building B-2A during shaking from the Tabas record with its strong component oriented in the building's X direction. Significant yielding does not occur in frames MF-4 to MF-6 that are oriented in the Y direction in either building.

4. GROUND MOTION SELECTION

Three sets of three-component ground motion records are selected for the study. They are the Sylmar record from the 17 January 1994, Northridge earthquake ($M_w = 6.7$), the Tabas record from the 16 September 1978, Iran earthquake ($M_w = 7.3$), and the Takatori record from the 17 January 1995, Kobe earthquake ($M_w = 6.9$). All three are near-source records with a distance to source of less than 5 km. The velocity histories and the pseudoacceleration response spectra of the two horizontal components of the three records are shown in Figure 4. Both the velocity and displacement histories consist of large amplitude, long period pulses [6]. The strong component of the Sylmar record has a 2.5 s period pulse with velocity amplitude exceeding 125 cm s^{-1} and displacement amplitude exceeding 30 cm. The corresponding numbers for the Tabas record strong component are a 5.5 s pulse with peak velocity amplitude exceeding 120 cm s^{-1}, and peak displacement exceeding 80 cm. For the Takatori record the near-source pulse has a period of about 2 s with peak velocity amplitude of 150 cm s^{-1}, and peak displacement amplitude of about 50 cm.

DOI: 10.1002/eqe

Table III. Stresses at the reentrant corners in the buildings.

		Stresses (psi)							
		Peak principal stresses in slab				Peak axial stress in moment-frame beams			
		Tensile		Compressive		Tensile		Compressive	
Building ID	Ground motion	Corner	Elsewhere	Corner	Elsewhere	Corner	Elsewhere	Corner	Elsewhere
B-1	Sylmar [X]*	286.1	194.1	322.0	207.5	3504.4	1951.8	3314.5	1888.1
	Sylmar [Y]†	279.9	183.8	291.5	199.3	2987.1	1816.1	2994.8	1875.8
	Tabas [X]*	471.1	276.9	569.0	278.6	4604.8	2899.9	4292.2	2352.5
	Tabas [Y]†	348.9	354.6	399.4	339.8	4278.13	3003.78	4021.3	1835.1
	Takatori [X]*	364.8	256.8	388.1	255.3	4160.8	2931.9	3979.5	1949.4
	Takatori [Y]†	391.4	245.0	401.2	247.8	3560.4	3053.4	3380.5	2175.6
B-2	Sylmar [X]*	209.7	223.6	246.4	431.8	2592.6	10707.2	2510.0	2191.7
	Tabas [X]*	249.0	257.4	298.8	496.5	10310.3	14221.8	2773.1	2361.1
	Takatori [X]*	221.7	258.7	306.7	264.3	3006.7	10154.9	3506.5	2577.9
B-2A	Sylmar [X]*	259.8	249.7	247.2	212.4	3006.3	2467.1	2184.8	1989.6
	Tabas [X]*	245.4	236.2	246.6	594.1	2957.7	12584.9	2287.2	1808.5
	Takatori [X]*	277.2	237.2	213.3	254.8	3850.11	6916.8	2404.1	2240.9

*Strong ground motion component in building's X direction.
†Strong ground motion component in building's Y direction.

The pulse periods are in the proximity of the fundamental periods of all the buildings (Table I). To quantify the distribution and extent of yielding due to these strong near-source pulses, finite-element models of all the buildings are analysed for three-component ground motion. For buildings that are not symmetric, two sets of analyses are performed—one with the strong horizontal component of the ground motion oriented in the building's X direction, and the other with the strong horizontal component oriented in the building's Y direction.

5. RESPONSE OF BUILDINGS WITH REENTRANT CORNERS

The peak roof displacement, peak interstorey drift ratios, and the permanent roof offset following the earthquake for each analysis case are given in Table II. Tabas is the most damaging of the three records to all three buildings while the Sylmar record is the least damaging. Peak interstorey drift ratios are at or exceed 0.05 in all three buildings under the Tabas and Takatori records while they are at about 0.03 under the Sylmar ground shaking. To put this in perspective, the FEMA-356 (Federal Emergency Management Agency) [11] drift limit for the collapse prevention performance level of existing buildings is 0.05 and the corresponding FEMA-350 [12] drift limit for new buildings is 0.06. None of the buildings would satisfy the life-safety performance level for existing buildings given by FEMA-356 (0.025) even under the Sylmar record. A permanent roof offset of about 0.9 m occurs in buildings B-1 and B-2 under the Tabas ground motion which corresponds to an

DOI: 10.1002/eqe

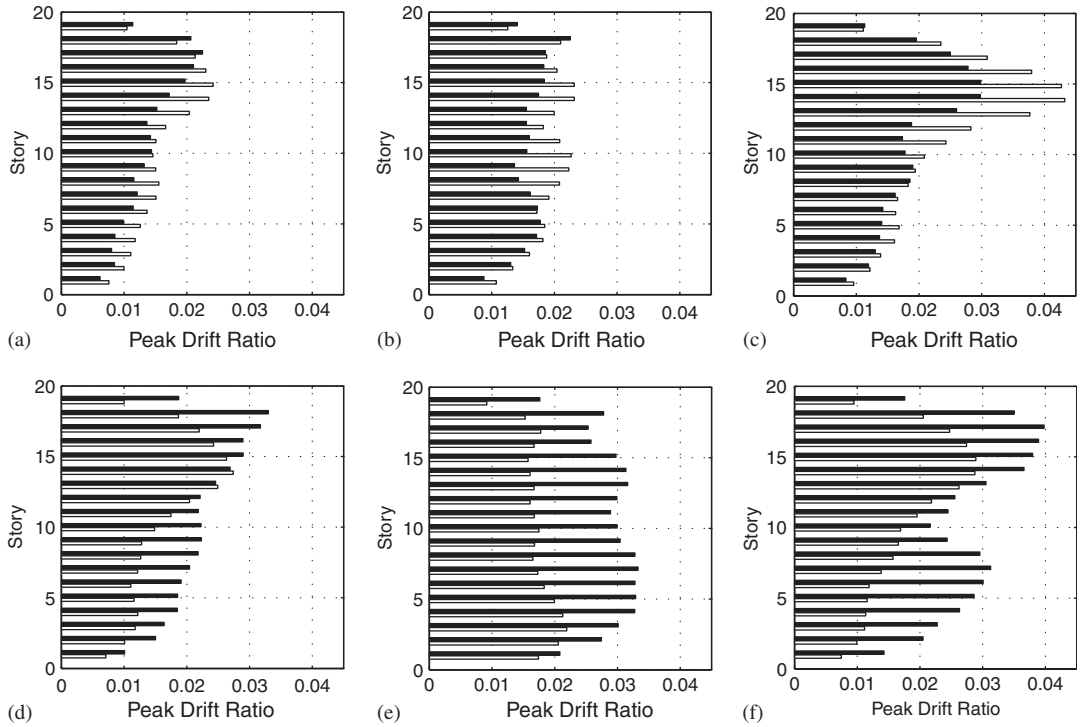

Figure 11. Building B-3 peak interstorey drifts (white bars represent X drifts and black bars represent Y drifts): (a)–(c) Sylmar, Tabas, and Takatori record strong components in building's X direction; and (d)–(f) Sylmar, Tabas, and Takatori record strong components in building's Y direction.

average inclination of about 1.25% in building B-1 and 1.15% in building B-2. This in itself would result in significant occupancy interruption. For example, following the Northridge earthquake an out of plumbness of about 15.2 cm (6 in) in an 18-storey steel moment-frame building (75.7 m) resulted in misalignment of elevators and downtime to undertake repairs [13]. The Takatori ground motion record results in slightly smaller permanent roof offsets, while the Sylmar record results in minimal permanent roof offsets.

The distribution of peak interstorey drift ratio over the height of building B-1 when subjected to the Sylmar, Tabas, and Takatori ground motion records is shown in Figure 5. The peak drift pattern when the strong component of each ground motion record is applied in the building's X direction is very similar to that when it is applied in the building's Y direction. This is probably because the dynamic characteristics of the building in the X and Y directions are very similar, as evidenced by the proximity of the natural periods in the two directions, even though the framing configurations in the two directions are quite different. The X direction peak drifts when the ground motion strong component is applied in the X direction are greater than the Y direction peak drifts when the strong component is oriented in the Y direction. The localization of damage in building B-1 when subjected to the Sylmar and Takatori records occurs in about the same regions over the height of the building as evidenced by an increase in the peak interstorey drift ratios in the vicinity of stories 8, 9, 16 and 17. The pulse period in the Sylmar and Takatori records is about the same

DOI: 10.1002/eqe

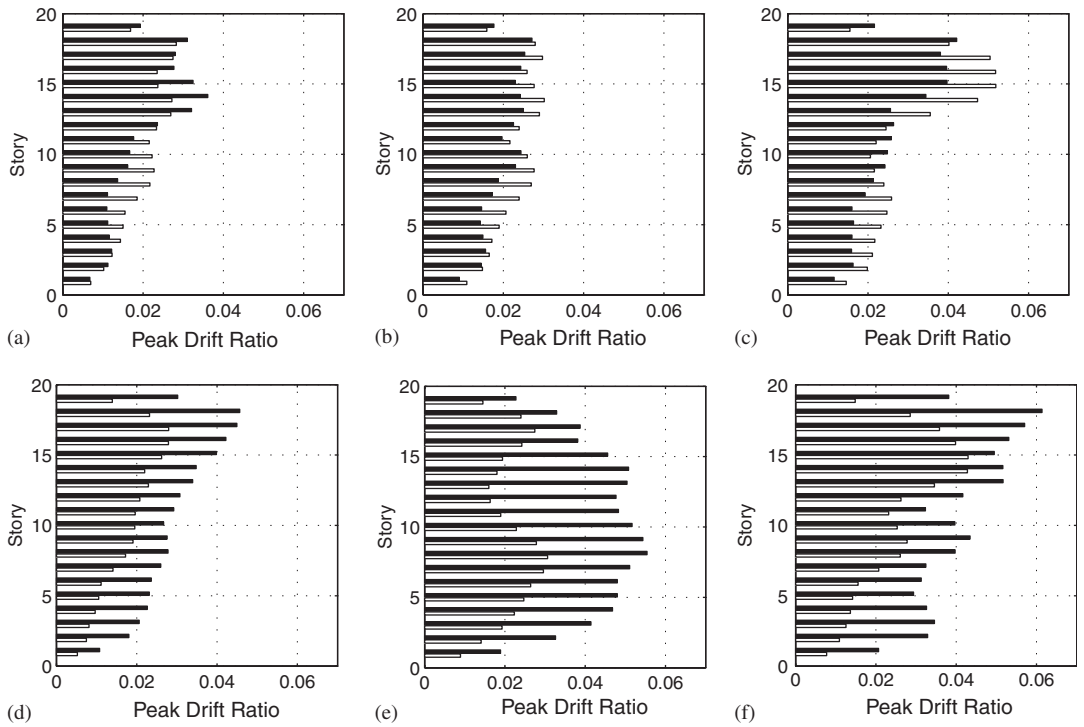

Figure 12. Building B-3A peak interstorey drifts (white bars represent X drifts and black bars represent Y drifts): (a)–(c) Sylmar, Tabas, and Takatori record strong components in building's X direction; and (d)–(f) Sylmar, Tabas, and Takatori record strong components in building's Y direction.

and this possibly results in similar damage localization patterns. When building B-1 is subjected to the Tabas record, damage localizes in a single region although it is spread over a greater number of stories. This is consistent with the fact that the wavelength of the near-source pulse in the Tabas record is more than twice of that in the Sylmar and Takatori records. The distribution of peak interstorey drift ratio over the heights of buildings B-2 and B-2A when subjected to the Sylmar, Tabas, and Takatori ground motion records is shown in Figure 6. Results are shown for the case of the strong component of the ground motion applied in the building X direction alone (since both buildings are symmetric). The observations made for building B-1 are applicable to buildings B-2 and B-2A as well. The peak drifts in building B-2A are only marginally greater than those in building B-2. This is because the lower stiffness of building B-2A, relative to building B-2, simultaneously results in a smaller seismic demand and the two effects approximately cancel each other.

Figure 7 shows the plastic rotations at ends of beams and columns, and panel zones in the moment-frames of building B-1 during shaking from the Tabas record with its strong horizontal component oriented in the building's X and Y directions. Damage is limited to the X direction frames in the analysis with the ground motion strong horizontal component in the X direction, and in the Y direction frames when the ground motion strong horizontal component is applied in the building's Y direction. Yielding is uniformly distributed amongst all the frames in a given

DOI: 10.1002/eqe

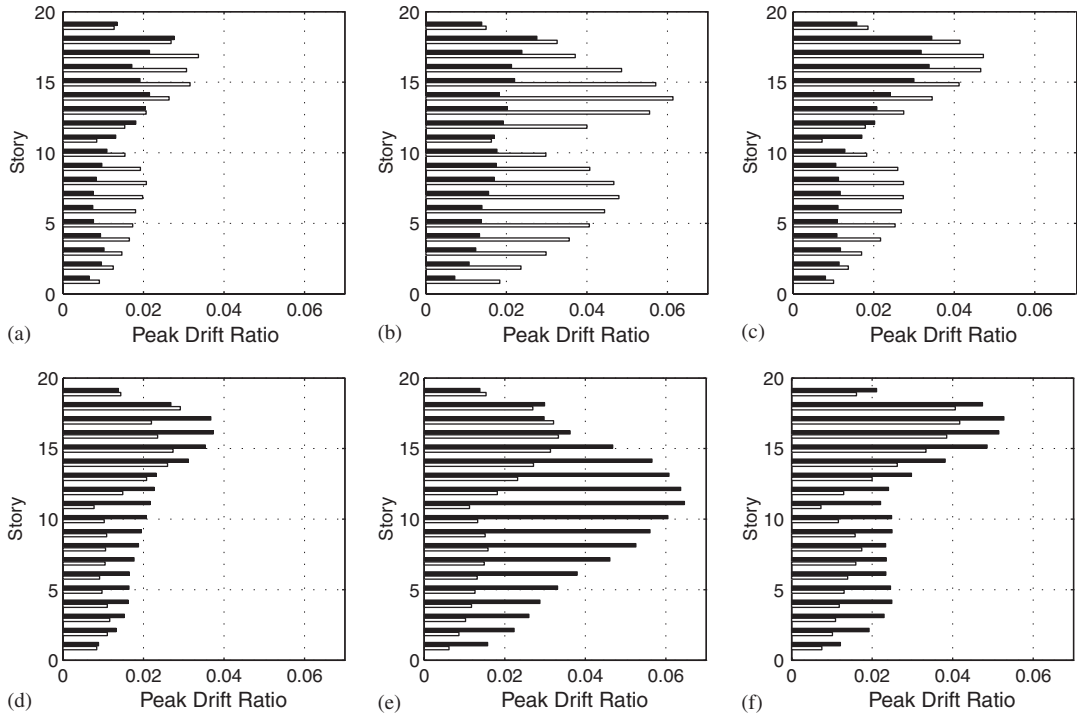

Figure 13. Building B-4 peak interstorey drifts (white bars represent X drifts and black bars represent Y drifts): (a)–(c) Sylmar, Tabas, and Takatori record strong components in building's X direction; and (d)–(f) Sylmar, Tabas, and Takatori record strong components in building's Y direction.

direction. This points to minimal twisting, if any, in the building response. In both analysis cases, the plastic rotation demand on the connections is up to 4% of a radian. Peak yielding occurs at level 9 and diminishes in a bell-shaped manner going away from this level to higher and lower levels. Building B-1 results for the Takatori ground motion record are presented in Figures 8 and 9. Similar to the Tabas ground motion analysis cases, the damage in the frames oriented in the direction of the ground motion strong component is equally distributed indicating that the building experienced little twisting, if any. However, the weak component of the Takatori ground motion is actually strong enough to induce yielding in the frames oriented in that direction. While this yielding is limited to the top third of the height of the frames (about level 17), the yielding in the frames oriented in the direction of the ground motion strong component gets localized in two distinct regions—the top third (about level 17) as well as the bottom half (about level 7) of the building. The peak yielding is limited to about 3% which is less than the demand imposed by the Tabas ground motion record.

Figure 10 shows a comparison of the plastic rotation in the X direction frames of buildings B-2 and B-2A when subjected to the Tabas record with the strong horizontal component oriented in the building's X direction. In building B-2 the 2-bay wing moment-frame, MF-3, was made very stiff to control wind drifts. During the ground motion analysis, the distribution of the lateral forces between this frame and the 5-bay moment frame, MF-1, is about the same resulting in greater

DOI: 10.1002/eqe

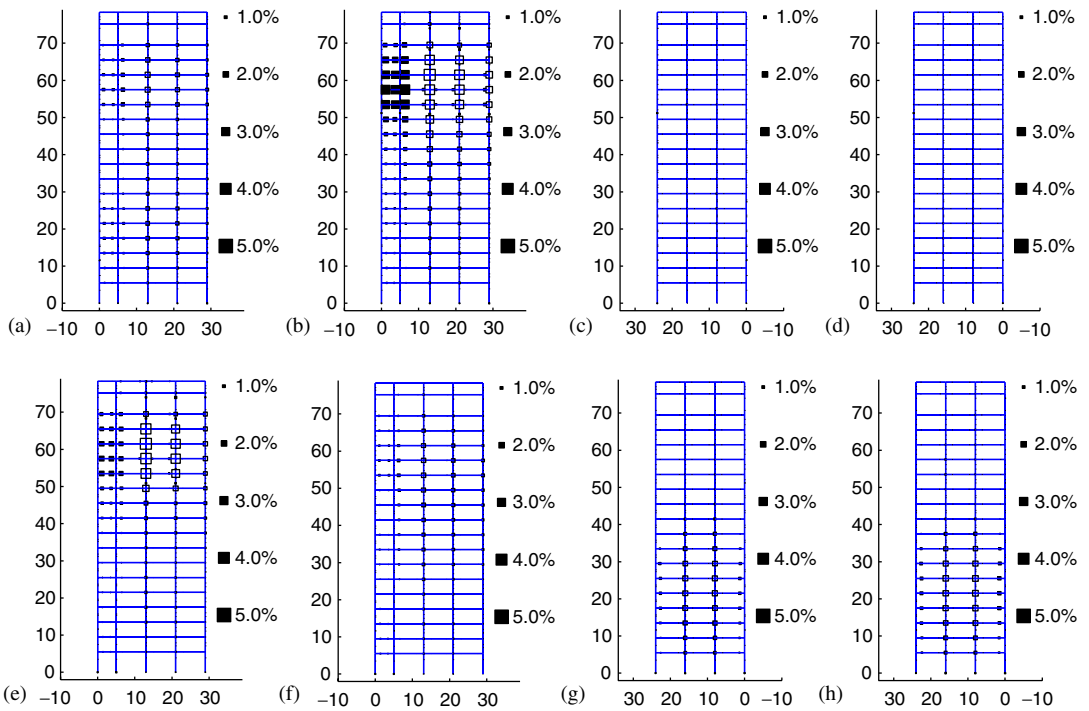

Figure 14. Plastic rotations at ends of beams and columns (black squares), and panel zones (white squares) in frames MF-1 to MF-4 of building B-3 during shaking from the Takatori record with its strong component oriented in the building's X direction ((a)–(d)), and Y direction ((e)–(h)).

yielding in its beams when compared to the more redundant MF-1. This demonstrates the effect of stiffness increase without a proportional increase in strength in frame MF-3. In building B-2A, on the other hand, the ratio of strength to stiffness in the various moment-frames is roughly the same resulting in a uniform yield distribution amongst all the frames oriented in the X direction. However, the lower strength of the frames in building B-2A leads to an overall increase in yielding.

To model stress concentrations at reentrant corners accurately, the floor slab in the proximity of the corner needs to be heavily discretized into nonlinear shell elements. In this analysis, however, the floor slab is modelled using elastic plane-stress elements with no special discretization at the reentrant corners. Stress concentration, if any, gets averaged over a large area. A large stress concentration may show up as a small increase in corner element stresses. Furthermore, elevator and stair openings are not modelled. Despite these limitations, this analysis may still provide some insight into the problem. Table III lists the peak stresses in the plane-stress elements, used to model the floor slabs in the three buildings, for each of the analysis cases. The peak tensile and compressive principal stresses at the elements that constitute the reentrant corner are compared against the corresponding stresses in the remaining elements used to model the floor slab. In addition, the peak axial stress in moment-frame beams at the reentrant corners is compared against that in moment-frame beams away from the corners. In neither case is a systematic stress

DOI: 10.1002/eqe

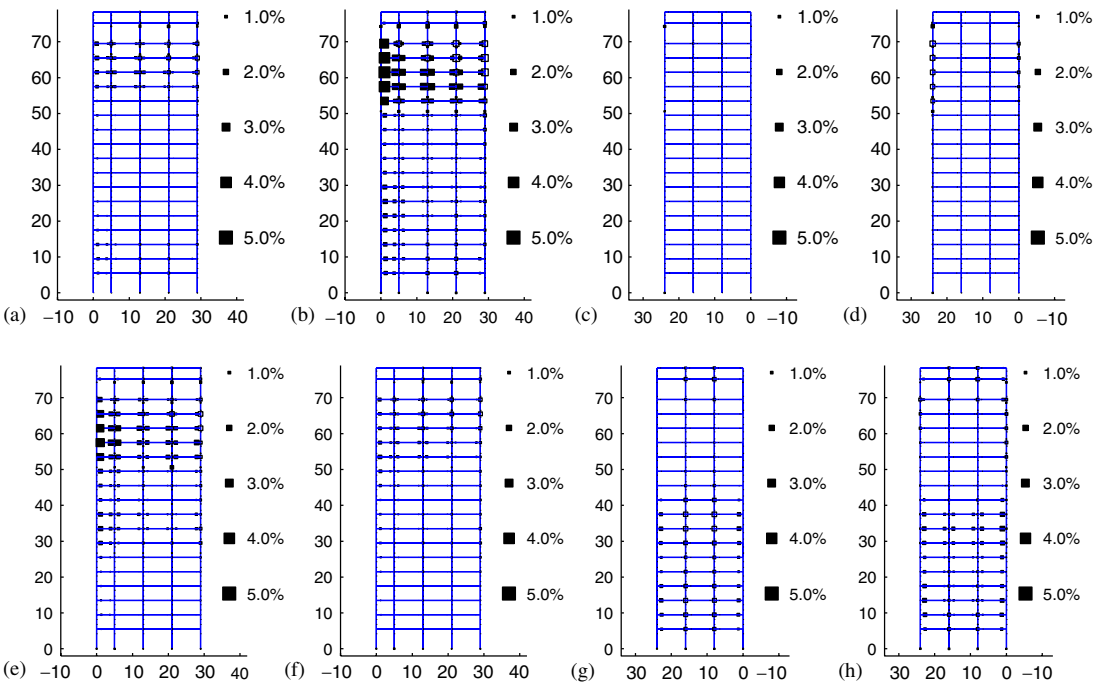

Figure 15. Plastic rotations at ends of beams and columns (black squares), and panel zones (white squares) in frames MF-1 to MF-4 of building B-3A during shaking from the Takatori record with its strong component oriented in the building's X direction ((a)–(d)), and Y direction ((e)–(h)).

concentration observed at the corner in the L-shaped buildings, B-2 and B-2A. However, there is an increase in the corners stresses in building B-1 when compared to stresses elsewhere in the slab. It is not clear whether this is a reentrant corner effect or the effect of the necking of the plan area at the corners. The single-bay overlap of the floor ties the two spines of the building together during an earthquake and this would naturally lead to an increase in the diaphragm stresses there. Having said this, a more rigorous and detailed analysis is required to conclusively rule out the incidence of stress concentration at the reentrant corners.

6. RESPONSE OF BUILDINGS WITH TORSIONAL ECCENTRICITY

The peak roof displacement, peak interstorey drift ratios, and the permanent roof offset in the three buildings with torsional eccentricity for each analysis case are given in Table II. While the Takatori record causes the greatest peak interstorey drifts in buildings B-3 and B-3A, both Tabas and Takatori records are equally severe on building B-4. In general, all three buildings seem weaker in the Y direction as evidenced by the consistently larger drifts when the strong components of the three records are oriented in the building's Y direction. This is primarily because the mass–stiffness

DOI: 10.1002/eqe

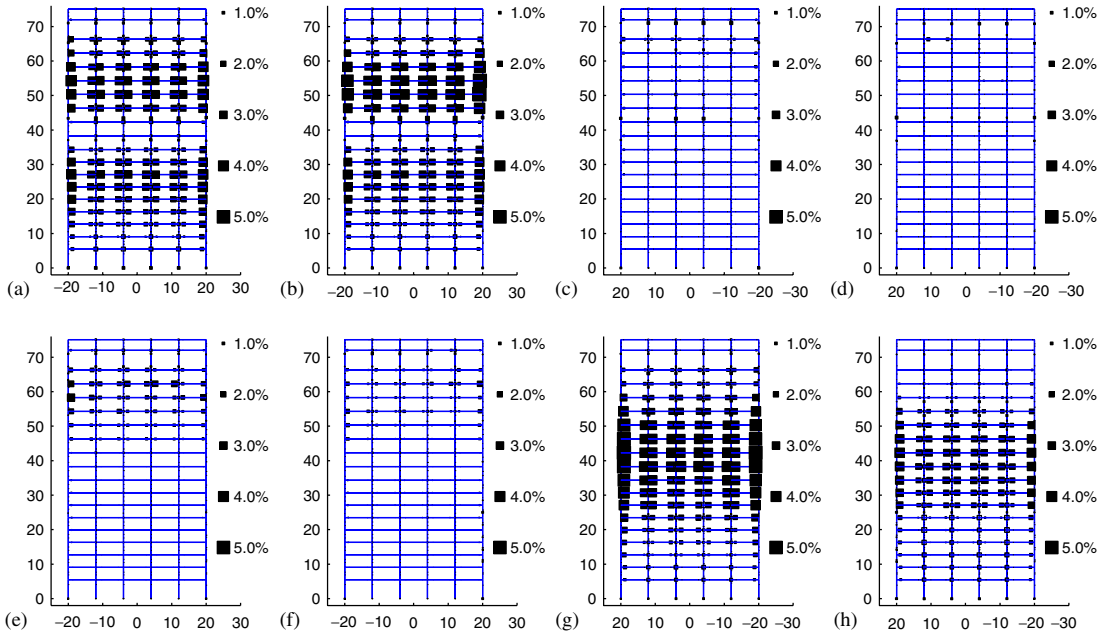

Figure 16. Plastic rotations at ends of beams and columns (black squares), and panel zones (white squares) in frames MF-1 to MF-4 of building B-4 during shaking from the Tabas record with its strong component oriented in the building's X direction ((a)–(d)), and Y direction ((e)–(h)).

eccentricity is unidirectional and causes twisting in the buildings under Y direction forcing. All three buildings fail to satisfy the life-safety performance criterion for existing buildings, a limit on the interstorey drift of 0.025, specified by the Federal Emergency Management Agency (FEMA) document FEMA-356 [11] for most of the analysis cases. Buildings B-3 and B-4 do not satisfy the collapse prevention criterion, a limit on the interstorey drift of 0.05, in three of the six analysis cases. Note that the collapse prevention criterion for new buildings specified in FEMA-350 [12] is more lenient, an interstorey drift limit of 0.06. The permanent roof offsets are quite low for buildings B-3 and B-3A (except for the Tabas case with its strong component oriented in the Y direction). It should be noted, however, that not all modes of failure have been included in these analyses. These include column local flange buckling and column splice tensile failure that could have the effect of worsening the building performance. The permanent tilt in building B-4 is greater than in B-3 and B-3A for each of the six analysis cases.

Figures 11–13 illustrate the distribution of peak interstorey drifts over the height of buildings B-3, B-3A, and B-4, respectively, for each of the six analysis cases. In each instance, the peak drift pattern in building B-3A is not significantly different from the corresponding pattern in building B-3, although the drift amplitudes are greater. The asymmetric stiffness in buildings B-3 and B-3A results in similar X and Y peak drifts when the strong component of the ground motion is oriented in the X direction, with the weak component of the ground motion causing sufficiently large drifts at the soft corners on the flexible face of the buildings. The difference in the intensities of the

DOI: 10.1002/eqe

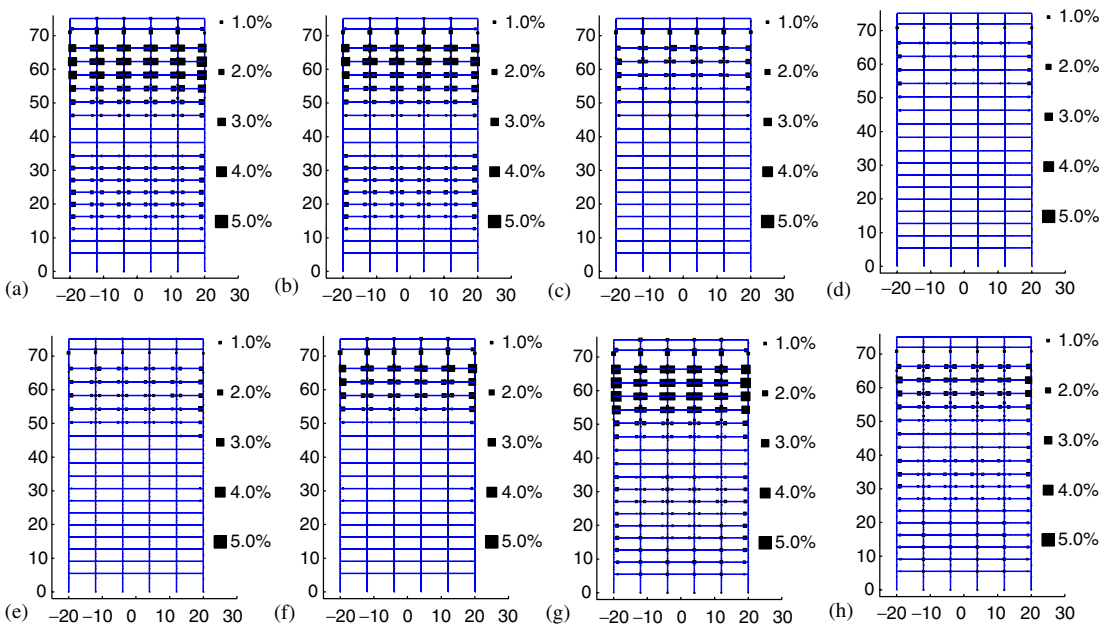

Figure 17. Plastic rotations at ends of beams and columns (black squares), and panel zones (white squares) in frames MF-1 to MF-4 of building B-4 during shaking from the Takatori record with its strong component oriented in the building's X direction ((a)–(d)), and Y direction ((e)–(h)).

ground motion in the two directions is equally balanced by the lower stiffness of the flexible face of the buildings in the Y direction. The difference in stiffness between the flexible and stiff Y direction faces of building B-4, however, is not as stark. Thus, in this case, the ground motion strong component when oriented in the building's X direction induces larger interstorey drifts in that direction when compared to the Y direction. Similar results can be seen in the building when the strong component of the ground motion is oriented in its Y direction, with greater yielding occurring in the Y direction frames. The stiff 11th storey transfer trusses that are oriented in the X direction in building B-4 dramatically reduce the peak interstorey drift at that storey and the stories immediately above and below. This is especially prominent in the cases where the strong component of the ground motion is oriented in the building X direction (see Figures 13(a)–(c)). In the absence of the transfer trusses, these peak interstorey drift patterns might have resembled the cases with the strong component oriented in the building's Y direction (Figures 13(d)–(f)).

The plastic rotations at the ends of beams and columns and the panel zones of the moment frames in building B-3 during shaking from the Takatori ground motion are shown in Figure 14 for the cases with the ground motion strong horizontal component oriented in the building's X and Y directions. Figure 15 illustrates the corresponding results for building B-3A. In both these buildings, twisting, caused by the eccentricity through which the Y direction inertial forces act, is resisted by the X direction moment-frames. Twisting adds to the direct stresses caused by the X direction ground motion in one of the X direction frames and negates/reduces the direct stresses in the other X direction frame, resulting in an unsymmetrical yield pattern in these frames. When

DOI: 10.1002/eqe

the strong component of the Takatori ground motion is oriented in the X direction, major yielding occurs in moment-frame MF-2. The difference in the extent of yielding between moment-frames MF-1 and MF-2 represents the contribution of twisting to the response of the building. Since the failure of MF-2 would result in a total loss in capacity for the building to resist torsion, the effective redundancy of the building can be considered to have been cut in half. The regions, over the height of the building, where yielding localizes in building B-3A are about the same as in building B-3. But yielding shifts from the panel zones in building B-3 to the ends of moment-frame beams in building B-3A. The reduction in beam sizes in building B-3A makes the panel zones relatively stronger moving the yielding into the beams. Interestingly, even though the plastic rotations in the panel zones of building B-3 are greater than the plastic rotations in the beams of building B-3A, building B-3A has larger peak interstorey drifts.

The plastic rotations in the moment-frames of building B-4 under the Tabas and Takatori ground motion records are illustrated in Figures 16 and 17. When the strong horizontal component of the ground motion is oriented in the building's X direction, yielding is more or less equally distributed amongst the X direction moment-frames, MF-1 and MF-2, with very little yielding in the Y direction frames. The weak component of neither the Tabas nor the Takatori ground motion is strong enough to induce twisting that is large enough to cause significantly different levels of yielding in the X direction frames. However, orienting the ground motion strong component in the building's Y direction causes significant twisting resulting in unequal yielding not only in the Y direction frames but also in the X direction frames. Irrespective of whether the major ground motion pulses are in the positive Y direction or the negative Y direction, torsional eccentricity in the building is such that the stresses from twisting will always add to the stresses from direct translational shaking in moment-frame MF-3 whereas they will always negate the stresses from direct translational shaking in moment-frame MF-4. Thus, in both the Takatori and Tabas ground motion analysis cases, yielding is greater in MF-3 than in MF-4 (see Figures 16(g) and (h), and 17(g) and (h)). On the other hand, the stresses in the X direction frames, which are algebraic sums of the direct stresses from X-translational shaking and the stresses from twisting that is generated by the Y direction shaking, could be such that either of the two X direction frames MF-1 or MF-2 could see greater yielding. Thus, while the Tabas ground motion results in greater yielding in MF-1 (Figures 16(a) and (b)), the Takatori ground motion results in greater yielding in MF-2 (Figures 17(a) and (b)). The positive effect of the X direction trusses in controlling the interstorey drifts locally is apparent in the yield pattern shown in Figures 16(a)–(d) and 17(a)–(d).

7. CONCLUDING REMARKS

Analyses of 19-storey irregular steel moment-frame buildings, designed in accordance with UBC97, indicate that near-source ground motion records from magnitude 6.7–7.3 earthquakes create drift demands of the order of 0.05 and plastic rotation demands of the order of 4–5% of a radian in the beam to column connections and/or the panel zones. Past experiments on large beam sections with pre-Northridge beam-to-column connections, which are prone to fracture, could realize plastic rotations of less than 3% of a radian only before fracturing [14]. In order for engineers to ensure that buildings constructed today are able to withstand such earthquakes, it is critical that the large plastic rotation demands on the idealized beam-to-column connections in this study are realized at least in laboratory tests on post-Northridge connections. Unfortunately, tests performed on unreinforced steel moment connections made using notch-tough weld metal

DOI: 10.1002/eqe

and improved welding practices indicate that these connections, built under laboratory conditions, could develop a maximum plastic rotation of only 2.6% of a radian [15]. Similarly, cyclic testing of steel moment connections rehabilitated with 'reduced beam section (RBS)' or 'welded haunch' procedures resulted in the development of a maximum plastic rotation of only about 2.7% of a radian [16]. In fact, the results of all tests performed on post-Northridge welded moment-frame connections, summarized in a state of the art report (FEMA-355D) on connection performance by FEMA [17], indicate that very few specimen could develop plastic rotations up to 5% of a radian. This reflects a big gap between the seismic demand on these structures under near-source earthquakes and their capacity as dictated by constructability of the beam–column assembly in the moment-frames. Finally, the analysis of the torsionally sensitive buildings clearly highlights the three-dimensional effects of irregular building response. Three-component ground motion induces yielding in frames that are oriented in the direction of the weak component of the ground motion as well. Moreover, twisting causes unequal yielding in the frames. These results illustrate the limits of applicability of linear analysis methods contained in the seismic codes under such adverse conditions.

ACKNOWLEDGEMENTS

I wish to gratefully acknowledge the support and guidance provided by my Ph.D. advisor Dr John F. Hall, Professor of Civil Engineering at the California Institute of Technology, during the course of this study. This study was funded in part by the California Institute of Technology. I wish to thank the editor and reviewers for valuable comments that enhanced the article.

REFERENCES

1. Iwan WD. Near-field considerations in specification of seismic design motions for structures. *Proceedings of the Tenth European Conference on Earthquake Engineering*, Vienna, Austria, August 28–September 2, 1994.
2. Hall JF, Heaton TH, Halling MW, Wald DJ. Near-source ground motion and its effects on flexible buildings. *Earthquake Spectra* 1995; **11**(4):569–605.
3. ICBO. *1997 Uniform Building Code*, vol. 2. International Conference of Building Officials: Whittier, California, U.S.A., 1997.
4. ICC. *International Building Code 2006*. International Code Council: Falls Church, Virginia, U.S.A.
5. Wilson EL, Habibullah A. ETABS—three dimensional analysis of building systems, *Users Manual*. Computers and Structures, Inc.: Berkeley, California, U.S.A., 1986.
6. Krishnan S. Three-dimensional nonlinear analysis of tall irregular steel buildings subject to strong ground motion. *EERL 2003-01* (http://caltecheerl.library.caltech.edu/361). Earthquake Engineering Research Laboratory, California Institute of Technology, Pasadena, California, U.S.A., 2003.
7. Krishnan S. FRAME3D—*A Program for Three-dimensional Nonlinear Time-history Analysis of Steel Buildings*: *User Guide*, *EERL 2003-03* (http://caltecheerl.library.caltech.edu/366). Earthquake Engineering Research Laboratory, California Institute of Technology, Pasadena, California, 2003.
8. FRAME3D website. http://www.frame3d.caltech.edu
9. Krishnan S, Hall JF. Modeling steel frame buildings in three dimensions—Part II: elastofiber beam element and examples. *Journal of Engineering Mechanics* (ASCE) 2006; **132**(4):359–374.
10. Krishnan S, Hall JF. Modeling steel frame buildings in three dimensions—Part I: panel zone and plastic hinge beam elements. *Journal of Engineering Mechanics* (ASCE) 2006; **132**(4):345–358.
11. FEMA. Prestandard and commentary for the seismic rehabilitation of buildings. *FEMA-356*. Federal Emergency Management Agency, U.S.A., 2000.
12. FEMA. Recommended seismic design criteria for new steel moment-frame buildings. *FEMA-350*. Federal Emergency Management Agency, U.S.A., 2000.

DOI: 10.1002/eqe

13. SAC. Analytical and field investigations of buildings affected by the Northridge earthquake of January 17, 1994—Part 2. *SAC 95-04*, Part 2, Structural Engineers Association of California, Applied Technology Council, and California Universities for Research in Earthquake Engineering, U.S.A., 1995.
14. Engelhardt MD, Husain AS. Cyclic-loading performance of welded flange-bolted web connections. *Journal of Structural Engineering* (ASCE) 1992; **119**(12):3537–3550.
15. Stojadinovic B, Goel SC, Lee KH, Margarian AG, Choi JH. Parametric tests on unreinforced steel moment connections. *Journal of Structural Engineering* (ASCE) 2000; **126**(1):40–49.
16. Uang CMU, Yu QS, Noel S, Gross J. Cyclic testing of steel moment connections rehabilitated with RBS or welded haunch. *Journal of Structural Engineering* (ASCE) 2000; **126**(1):57–68.
17. FEMA. State of the art report on connection performance. *FEMA-355D*. Federal Emergency Management Agency, U.S.A., 2000.

DOI: 10.1002/eqe